FAST NEURAL NETWORK ADAPTATION VIA PARAMETER REMAPPING AND ARCHITECTURE SEARCH

Jiemin Fang[1][*][†] **Yuzhu Sun**[1][*][†]**, Kangjian Peng**[2][*]**, Qian Zhang**[2]**, Yuan Li**[2]**,**
Wenyu Liu[1]**, Xinggang Wang**[1][‡]
[1]School of EIC, Huazhong University of Science and Technology   [2]Horizon Robotics
{jaminfong, yzsun, liuwy, xgwang}@hust.edu.cn
{kangjian.peng, qian01.zhang, yuan.li}@horizon.ai

ABSTRACT

Deep neural networks achieve remarkable performance in many computer vision tasks. Most state-of-the-art (*SOTA*) semantic segmentation and object detection approaches reuse neural network architectures designed for image classification as the backbone, commonly pre-trained on ImageNet. However, performance gains can be achieved by designing network architectures specifically for detection and segmentation, as shown by recent neural architecture search (NAS) research for detection and segmentation. One major challenge though, is that ImageNet pre-training of the search space representation (a.k.a. super network) or the searched networks incurs huge computational cost. In this paper, we propose a Fast Neural Network Adaptation (FNA) method, which can adapt both the architecture and parameters of a seed network (e.g. a high performing manually designed backbone) to become a network with different depth, width, or kernels via a Parameter Remapping technique, making it possible to utilize NAS for detection/segmentation tasks a lot more efficiently. In our experiments, we conduct FNA on MobileNetV2 to obtain new networks for both segmentation and detection that clearly out-perform existing networks designed both manually and by NAS. The total computation cost of FNA is significantly less than *SOTA* segmentation/detection NAS approaches: $1737\times$ less than DPC, $6.8\times$ less than Auto-DeepLab and $7.4\times$ less than DetNAS. The code is available at https://github.com/JaminFong/FNA.

1 INTRODUCTION

Deep convolutional neural networks have achieved great successes in computer vision tasks such as image classification (Krizhevsky et al., 2012; He et al., 2016; Howard et al., 2017), semantic segmentation (Long et al., 2015; Ronneberger et al., 2015; Chen et al., 2017b) and object detection (Ren et al., 2015; Liu et al., 2016; Lin et al., 2017) etc. Image classification has always served as a fundamental task for neural architecture design. It is common to use networks designed and pre-trained on the classification task as the backbone and fine-tune them for segmentation or detection tasks. However, the backbone plays an important role in the performance on these tasks and the difference between these tasks calls for different design principles of the backbones. For example, segmentation tasks require high-resolution features and object detection tasks need to make both localization and classification predictions from each convolutional feature. Such distinctions make neural architectures designed for classification tasks fall short. Some attempts (Li et al., 2018; Wang et al., 2019) have been made to tackle this problem.

Handcrafted neural architecture design is inefficient, requires a lot of human expertise, and may not find the best-performing networks. Recently, neural architecture search (NAS) methods (Zoph et al., 2017; Pham et al., 2018; Liu et al., 2018) see a rise in popularity. Some works (Liu et al.,

---

[*]Equal contributions.

[†]The work is performed during an internship at Horizon Robotics.
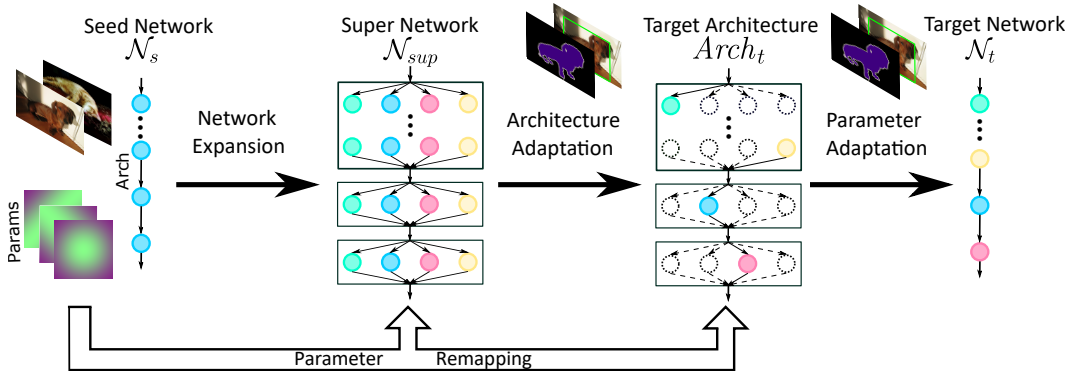
[‡]Corresponding author.

Figure 1: The framework of our proposed FNA. Firstly, we select an artificially designed network as the seed network $\mathcal{N}_s$ and expand $\mathcal{N}_s$ to a super network $\mathcal{N}_{sup}$ which is the representation of the search space. Then parameters of $\mathcal{N}_s$ are remapped to $\mathcal{N}_{sup}$. We utilize the NAS method to start the architecture adaptation with the super network and obtain the target architecture $Arch_t$. Before parameter adaptation, we remap the parameters of $\mathcal{N}_s$ to $Arch_t$. Finally, we adapt the parameters of $Arch_t$ to get the target network $\mathcal{N}_t$.

2019a; Zhang et al., 2019; Chen et al., 2019b) propose to use NAS to design backbone architectures specifically for segmentation or detection tasks. Nevertheless, pre-training remains a inevitable but costly procedure. Though some (He et al., 2018) recently demonstrates that pre-training is not always necessary for accuracy considerations, training from scratch on the target task still takes more iterations than fine-tuning from a pre-trained model. For NAS methods, the pre-training cost is non-negligible for evaluating the networks in the search space. One-shot search methods (Brock et al., 2017; Bender et al., 2018; Chen et al., 2019b) integrate all possible architectures in one super network but pre-training the super network and the searched network still bears huge computation cost.

As ImageNet (Deng et al., 2009) pre-training has been a standard practice for many computer vision tasks, there are lots of models trained on ImageNet available in the community. To take full advantages of these models, we propose a Fast Neural Network Adaptation (FNA) method based on a novel parameter remapping paradigm. Our method can adapt both the architecture and parameters of one network to a new task with negligible cost. Fig. 1 shows the whole framework. The adaptation is performed on both the architecture- and parameter-level. We adopt the NAS methods (Zoph et al., 2017; Real et al., 2018; Liu et al., 2019b) to implement the architecture-level adaptation. We select a manually designed network (MobileNetV2 (Sandler et al., 2018) in our experiments) as the `seed network`, which is pre-trained on ImageNet. Then, we expand the seed network to a super network which is the representation of the search space in FNA. New parameters in the super network are initialized by mapping those from the seed network using parameter remapping. Thanks to that, the neural architecture search can be performed efficiently on the detection and segmentation tasks. With FNA we obtain a new optimal target architecture for the new task. Similarly, we remap the parameters of the seed network to the target architecture for initialization and fine-tune it on the target task with no need of pre-training on a large-scale dataset.

We demonstrate FNA's effectiveness and efficiency via experiments on both segmentation and detection tasks. We adapt the manually designed network MobileNetV2 (Sandler et al., 2018) to segmentation framework DeepLabv3 (Chen et al., 2017b), detection framework RetinaNet (Lin et al., 2017) and SSDLite (Liu et al., 2016; Sandler et al., 2018). Networks adapted by FNA surpass both manually designed and NAS searched networks in terms of both performance and model MAdds. Compared to NAS methods, FNA costs $1737\times$ less than DPC (Chen et al., 2018a), $6.8\times$ less than Auto-DeepLab (Liu et al., 2019a) and $7.4\times$ less than DetNAS (Chen et al., 2019b).

2 RELATED WORK

Neural Architecture Search With reinforcement learning (RL) and evolutionary algorithm (EA) being applied to NAS methods, many works (Zoph & Le, 2016; Zoph et al., 2017; Real et al., 2018)

make great progress in promoting the performances of neural networks. Recently, NAS methods based on one-shot model (Brock et al., 2017; Bender et al., 2018) or differentiable representations (Liu et al., 2019b; Cai et al., 2019; Fang et al., 2019b) achieve remarkable results with low search cost. We use the differentiable NAS method to implement architecture adaptation, which adjusts the architecture of the backbone network automatically.

Backbone Design   As deep neural network designing (Simonyan & Zisserman, 2014; Szegedy et al., 2016; He et al., 2016) develops, the backbones of segmentation or detection networks evolve accordingly. Some works improve the backbone architectures by modifying existing networks. PeleeNet (Wang et al., 2018) proposes a variant of DenseNet (Huang et al., 2017) for more real-time object detection on mobile devices. DetNet (Li et al., 2018) applies dilated convolution (Yu & Koltun, 2016) in the backbone to enlarge the receptive field which helps to detect objects. BiSeNet (Yu et al., 2018) and HRNet (Wang et al., 2019) design multiple paths to learn both high- and low- resolution representations for better dense prediction.

Parameter Remapping   Net2Net (Chen et al., 2015) proposes the function-preserving transformations to remap the parameters of one network to a new deeper or wider network. This remapping mechanism accelerates the training of the new larger network and achieves great performances. Following this manner, EAS (Cai et al., 2018) extends the parameter remapping concept to neural architecture search. Moreover, some NAS works (Pham et al., 2018; Fang et al., 2019a; Elsken et al., 2019) apply parameters sharing on child models to accelerate the search process. Our parameter remapping paradigm extends the mapping dimension with the kernel level. Parameters can be also mapped to a shallower or narrower network with our scheme, while Net2Net focuses on mapping parameters to a deeper and wider network. The parameter remapping in our FNA largely decreases the computation cost of the network adaptation by taking full advantages of the ImageNet pre-trained parameters.

3   METHOD

As the most commonly used network for designing search spaces in NAS methods (Tan et al., 2018; Cai et al., 2019; Fang et al., 2019b), MobileNetV2 (Sandler et al., 2018) is selected as the seed network to give the details of our method. To adapt the network to segmentation and detection tasks, we adjust the architecture elements on three levels, i.e., convolution kernel size, depth and width of the network. In this section, we first describe the parameter remapping paradigm. Then we explain the whole procedure of the network adaptation.

3.1   PARAMETER REMAPPING

We define *parameter remapping* as one paradigm which aims at mapping the parameters of one seed network to another one. We denote the seed network as $\mathcal{N}_s$ and the new network as $\mathcal{N}_n$, whose parameters are denoted as $\boldsymbol{W}_s$ and $\boldsymbol{W}_n$ respectively. The remapping paradigm is illustrated in the following three aspects. The remapping on the depth-level is firstly carried out and then the remapping on the kernel- and width- level is conducted simultaneously. Moreover, we study different remapping strategies in the experiments (Sec. 4.5).

Remapping on Depth-level   We introduce more depth settings in our architecture adaptation process. In other word, we adjust the number of inverted residual blocks (MBConvs) (Sandler et al., 2018) in every stage of the network. We assume that one stage in the seed network $\mathcal{N}_s$ has l layers. The parameters of each layer can be denoted as $\{\boldsymbol{W}_s^{(1)}, \boldsymbol{W}_s^{(2)}, \ldots, \boldsymbol{W}_s^{(l)}\}$. Similarly, we assume that the corresponding stage with m layers in the new network $\mathcal{N}_n$ has parameters $\{\boldsymbol{W}_n^{(1)}, \boldsymbol{W}_n^{(2)}, \ldots, \boldsymbol{W}_n^{(m)}\}$. The remapping process on the depth-level is shown in Fig. 2(a). The parameters of layers in $\mathcal{N}_n$ which also exit in $\mathcal{N}_s$ are just copied from $\mathcal{N}_s$. The parameters of new layers are all copied from the last layer in the stage of $\mathcal{N}_s$. It is formulated as

$$
\begin{aligned}
f(i) &= min(i, l), \\
W_n^{(i)} &= W_s^{(f(i))}, \quad \forall 1 \le i \le m.
\end{aligned}
\tag{1}
$$

Remapping on Width-level   In the MBConv block of MobileNetV2 (Sandler et al., 2018) network, the first point-wise convolution expands the low-dimensional features to a high dimension.

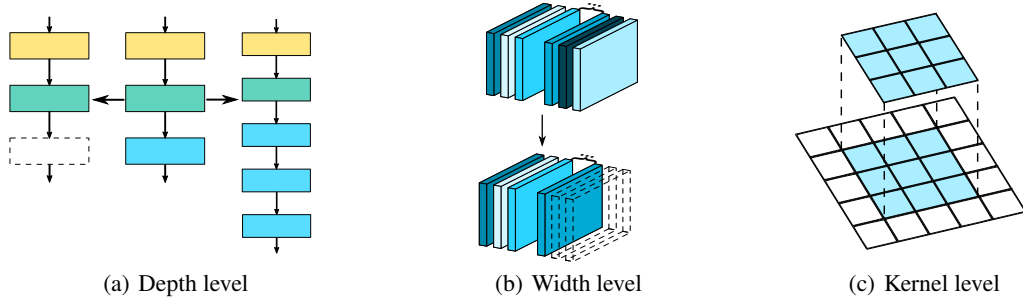(a) Depth level   (b) Width level   (c) Kernel level

Figure 2: Our parameters are remapped on three levels. (a) shows the depth-level remapping. The parameters of existing corresponding layers are mapped from the original network. The parameters of new layers are mapped from the last layer in the original network. (b) shows the width-level remapping. For each channels-diminished dimension, the parameters are copied from the original existing ones. (c) shows the kernel-level remapping. The original parameters are mapped to the central part of the new larger kernel. The values of the other parameters are assigned with 0.

This practice can be utilized for expanding the width and capacity of one neural network. We allow smaller expansion ratios for architecture adaptation. We denote the parameters of one convolution in $\mathcal{N}_s$ as $\boldsymbol{W}^s \in \mathbb{R}^{p \times q \times h \times w}$ and that in $\mathcal{N}_n$ as $\boldsymbol{W}^n \in \mathbb{R}^{r \times s \times h \times w}$, where $r \leq p$ and $s \leq q$. As shown in Fig. 2(b), on the width-level, we directly map the first r or s channels of parameters in $\mathcal{N}_s$ to the narrower one in $\mathcal{N}_n$. It can be formulated as

$$\boldsymbol{W}^n_{i,j,:,:} = \boldsymbol{W}^s_{i,j,:,:}, \quad \forall 1 \leq i \leq r, 1 \leq j \leq s. \tag{2}$$

Remapping on Kernel-level The kernel size is commonly set as 3×3 in most artificially-designed networks. To expand the receptive field and capture abundant features in segmentation or detection tasks, we introduce larger kernel size settings in the adaptation process. As Fig. 2(c) shows, to expand the 3×3 kernel to a larger one, we assign the parameters of the central 3×3 region in the large kernel with the values of the original 3×3 kernel. The values of the other region surrounding the central part are assigned with 0. We denote the parameters of the original 3×3 kernel as $\boldsymbol{W}^{3 \times 3}$ and the larger $k \times k$ kernel as $\boldsymbol{W}^{k \times k}$. The remapping process on kernel-level can be formulated as follows,

$$\boldsymbol{W}^{k \times k}_{:,:,h,w} = \begin{cases} \boldsymbol{W}^{3 \times 3}_{:,:,h,w} & \text{if} (k-3)/2 < h, w \leq (k+3)/2 \\ 0 & \text{otherwise} \end{cases}, \tag{3}$$

where h, w denote the indices of the spatial dimension. This design principle conforms to the function-preserving concept (Chen et al., 2015), which accelerates and stabilizes the optimization of the new network.

3.2 NEURAL NETWORK ADAPTATION

We divide our neural network adaptation into three steps. Fig. 1 demonstrates the whole adaptation procedure. Firstly, we expand the seed network to a super network which is the representation of the search space in the latter architecture adaptation process. Secondly, we perform the differentiable NAS method to implement network adaptation on the architecture-level and obtain the target architecture $Arch_t$. Finally, we adapt the parameters of the target architecture and obtain the target network $\mathcal{N}_t$. The aforementioned parameter remapping mechanism is deployed before the two stages, i.e. architecture adaptation and parameter adaptation.

Network Expansion We expand the seed network to a super network by introducing more options for architecture elements. For every MBConv layer, we allow for more kernel size settings $\{3, 5, 7\}$ and more expansion ratios $\{3, 6\}$. As most differentiable NAS methods (Liu et al., 2019b; Cai et al., 2019; Wu et al., 2018) do, we relax every layer as a weighted sum of all candidate operations.

$$\bar{o}^{(i)}(x) = \sum_{o \in O} \frac{exp(\alpha_o^{(i)})}{\sum_{o' \in O} exp(\alpha_{o'}^{(i)})} o(x), \tag{4}$$

Table 1: Semantic segmentation results on Cityscapes. OS: output stride, the spatial resolution ratio of input image to backbone output. The result of DPC in the brackets is our implemented version under the same settings as FNA. The MAdds of the models are computed with the 1024×2048 input resolution.

Method		OS	iters	Params	MAdds	mIOU(%)
MobileNetV2 (Sandler et al., 2018)				2.57M	24.52B	75.5
DPC (Chen et al., 2018a)	DeepLabv3	16	100K	2.51M	24.69B	75.4(75.7)
FNA				2.47M	24.17B	**76.6**
Auto-DeepLab-S (Liu et al., 2019a)		8	500K	10.15M	333.25B	75.2
FNA	DeepLabv3+	16	100K	5.71M	210.11B	77.2
FNA		8	100K	5.71M	313.87B	**78.0**

Table 2: Comparisons of computational cost on the semantic segmentation tasks. ArchAdapt: Architecture Adaptation. ParamAdapt: Parameter Adaptation. GHs: GPU Hours. $*$ indicates the computational cost calculated under our reproducing settings. $\dagger$ indicates the cost estimated according to the description in the original paper.

Method	Total Cost	ArchAdapt Cost	ParamAdapt Cost
DPC (Chen et al., 2018a)	62.2K GHs	62.2K GHs	30.0* GHs
Auto-DeepLab-S (Liu et al., 2019a)	244.0 GHs	72.0 GHs	172.0† GHs
FNA	35.8 GHs	1.4 GHs	34.4 GHs

where O denotes the operation set, α_o^i denotes the architecture parameter of operation o in the ith layer, and x denotes the input tensor. We set more layers in one stage of the super network and add the identity connection to the candidate operation set for depth search. After expanding the seed network to a super network, we remap the parameters of the seed network to the super network based on the paradigm illustrated in Sec. 3.1. This remapping strategy prevents the huge cost of ImageNet pre-training involved in the search space, i.e. the super network in differentiable NAS.

Architecture Adaptation We start the differentiable NAS process with the expanded super network directly on the target task, e.g., semantic segmentation or object detection. We first fine-tune operation weights of the super network for some epochs on the training dataset. After the weights are sufficiently trained, we start alternating the optimization of operation weights w with $\frac{\partial \mathcal{L}}{\partial w}$ and architecture parameters α with $\frac{\partial \mathcal{L}}{\partial \alpha}$. To accelerate the search process and decouple the parameters of different sub-networks, we only sample one path in each iteration according to the distribution of architecture parameters for operation weight updating. As the search process terminates, we use the architecture parameters α to derive the target architecture.

Parameter Adaptation We obtain the target architecture $Arch_t$ from architecture adaptation. To accommodate the new segmentation or detection tasks, the target architecture becomes different from that of the seed network $\mathcal{N}_s$ (which is primitively designed for the image classification task). Unlike conventional training strategy, we discard the cumbersome pre-training process of $Arch_t$ on ImageNet. We remap the parameters of $\mathcal{N}_s$ to $Arch_t$ utilizing the method described in Sec. 3.1. Finally, we directly fine-tune $Arch_t$ on the target task and obtain the final target network $\mathcal{N}_t$.

4 EXPERIMENTS

We select the ImageNet pre-trained MobileNetV2 model as the seed network and apply our FNA method on both semantic segmentation and object detection tasks. In this section, we firstly give the implementation details of our experiments; then we report and analyze the network adaptation results; finally, we perform ablation studies to validate the effectiveness of the parameter remapping paradigm and compare different parameter remapping implementations.

4.1 NETWORK ADAPTATION ON SEMANTIC SEGMENTATION

The semantic segmentation experiments are conducted on the Cityscapes (Cordts et al., 2016) dataset. In the architecture adaptation process, we map the seed network to the super network,

Table 3: Object detection results on MS-COCO. The MAdds are calculated with 1088×800 input.

Method		Params	MAdds	mAP(%)
ShuffleNetV2-20 (Chen et al., 2019b)		13.19M	132.76B	32.1
MobileNetV2 (Sandler et al., 2018)	RetinaNet	11.49M	133.05B	32.8
DetNAS (Chen et al., 2019b)		13.41M	133.26B	33.3
FNA		11.73M	133.03B	**33.9**
MobileNetV2 (Sandler et al., 2018)		4.3M	0.8B	22.1
Mnasnet-92 (Tan et al., 2018)	SSDLite	5.3M	1.0B	22.9
FNA		4.6M	0.9B	**23.3**

Table 4: Comparison of computational cost on the object detection tasks. All our experiments on object detection are conducted on TITAN-Xp GPUs.

Method	Total Cost	Super Network			Target Network	
		Pre-training	Finetuning	Search	Pre-training	Finetuning
DetNAS (Chen et al., 2019b)	68 GDs	12 GDs	12 GDs	20 GDs	12 GDs	12 GDs
FNA (RetinaNet)	9.2 GDs	-	-	6 GDs	-	3.2 GDs
FNA (SSDLite)	21.6 GDs	-	-	6.6 GDs	-	15 GDs

which is used as the backbone of DeepLabv3 (Chen et al., 2017b). We randomly sample 20% images from the training set as the validation set for architecture parameters updating. The original validation set is not used in the search process. To optimize the MAdds of the searched network, we define the loss function in search as $\mathcal{L} = \mathcal{L}_{task} + \lambda \log_\tau(cost)$. The first term denotes the cross-entropy loss and the second term controls the MAdds of the network. We set λ as 9×10^{-3} and τ as 45. The search process takes 80 epochs in total. The architecture optimization starts after 30 epochs. The whole search process is conducted on a single V100 GPU and takes only 1.4 hours in total.

In the parameter adaptation process, we remap the parameters of original MobileNetV2 to the target architecture obtained in the aforementioned architecture adaptation. The whole parameter adaptation process is conducted on 4 TITAN-Xp GPUs and takes 100K iterations, which cost only 8.5 hours in total.

Our semantic segmentation results are shown in Tab. 1. The FNA network achieves 76.6% mIOU on Cityscapes with the DeepLabv3 (Chen et al., 2017b) framework, 1.1% mIOU better than the manually designed seed Network MobileNetV2 (Sandler et al., 2018) with fewer MAdds. Compared with a NAS method DPC (Chen et al., 2018a) (with MobileNetV2 as the backbone) which searches a multi-scale module for semantic segmentation tasks, FNA gets 0.9% mIOU promotion with 0.52B fewer MAdds. For fair comparison with Auto-DeepLab (Liu et al., 2019a) which searches the backbone architecture on DeepLabv3 and retrains the searched network on DeepLabv3+ (Chen et al., 2018b), we adapt the parameters of the target architecture $Arch_t$ to DeepLabv3+ framework. Comparing with Auto-DeepLab-S, FNA achieves far better mIOU with fewer MAdds, Params and training iterations. With the remapping mechanism, FNA only takes 35.8 GPU hours, $1737\times$ less than DPC and $6.8\times$ less than Auto-DeepLab.

4.2 NETWORK ADAPTATION ON OBJECT DETECTION

We further implement our FNA method on object detection tasks. We adapt the MobileNetV2 seed network to two commonly used detection systems, RetinaNet (Lin et al., 2017) and a lightweight one SSDLite (Liu et al., 2016; Sandler et al., 2018). The experiments are conducted on the MS-COCO dataset (Lin et al., 2014b). Our implementation is based on the MMDetection (Chen et al., 2019a) framework. In the search process of architecture adaptation, we randomly sample 50% data from the original `trainval35k` set as the validation set.

We show the results on the COCO dataset in Tab. 3. In the RetinaNet framework, compared with two manually designed networks, ShuffleNetV2-10 (Ma et al., 2018; Chen et al., 2019b) and MobileNetV2 (Sandler et al., 2018), FNA achieves higher mAP with similar MAdds. Compared with DetNAS (Chen et al., 2019b) which searches the backbone of detection network, FNA achieves 0.6% higher mAP with 1.64M fewer Params and 0.2B fewer MAdds. As shown in Tab. 4, our total computation cost is only 13.5% of DetNAS. Moreover, we implement our FNA method on the SSDLite framework. In Tab. 3, FNA surpasses both the manually designed network MobileNetV2 and the NAS-searched network MnasNet-92, where MnasNet (Tan et al., 2018) takes around 3.8K GPU

days to search for the backbone network on ImageNet. The specific cost FNA takes on SSDLite is shown in Tab. 4. It is difficult to train the small network due to the simplification (Liu et al., 2019c). Therefore, experiments on SSDLite need long training schedule and take larger computation cost. The experimental results further demonstrate the efficiency and effectiveness of direct adaptation on the target task with parameter remapping.

4.3 Effectiveness of Parameter Remapping

To evaluate the effectiveness of the parameter remapping paradigm in our method, we attempt to optionally remove the parameter remapping process before the two stages, i.e. architecture adaptation and parameter adaptation. The experiments are conducted with the DeepLabv3 (Chen et al., 2017b) semantic segmentation framework on the Cityscapes dataset (Cordts et al., 2016).

Table 5: Effectiveness evaluation of Parameter Remapping. The experiments are conducted with DeepLabv3 on Cityscapes. Remap: Parameter Remapping. ArchAdapt: Architecture Adaptation. RandInit: Random Initialization. Pretrain: ImageNet Pretrain. ParamAdapt: Parameter Adaptation.

Row Num	Method	MAdds(B)	mIOU(%)
(1)	Remap → ArchAdapt → Remap → ParamAdapt (FNA)	24.17	**76.6**
(2)	RandInit → ArchAdapt → Remap → ParamAdapt	24.29	76.0
(3)	Remap → ArchAdapt → RandInit → ParamAdapt	24.17	73.0
(4)	RandInit → ArchAdapt → RandInit → ParamAdapt	24.29	72.4
(5)	Remap → ArchAdapt → Retrain → ParamAdapt	24.17	76.5

In Row (2) we remove the parameter remapping process before architecture adaptation. In other word, the search is performed from scratch without using the pre-trained network. The mIOU in Row (2) drops by 0.6% compared to FNA in Row (1). Then we remove the parameter remapping before parameter adaptation in Row (3), i.e. training the target architecture from scratch on the target task. The mIOU decreases by 3.6% compared the result of FNA. When we remove the parameter remapping before both stages in Row (4), it gets the worst performance. In Row (5), we first pretrain the searched architecture on ImageNet and then fine-tune it on the target task. It is worth noting that FNA even achieves a higher mIOU by a narrow margin (0.1%) than the ImageNet pre-trained one in Row (5). We conjecture that this may benefit from the regularization effect of parameter remapping before the parameter adaptation stage.

All the experiments are conducted using the same searching and training settings for fair comparisons. With parameter remapping applied on both stages, the adaptation achieves the best results in Tab. 5. Especially, the remapping process before parameter adaptation tends to provide greater performance gains than the remapping before architecture adaptation. All the experimental results demonstrate the importance and effectiveness of the proposed parameter remapping scheme.

Table 6: Results of random search experiments with the RetinaNet framework on MS-COCO. DiffSearch: Differentiable NAS. RandSearch: Random Search. The other definitions of abbreviations are the same as Tab. 5.

Row Num	Method	MAdds(B)	mAP(%)
(1)	DetNAS (Chen et al., 2019b)	133.26	33.3
(2)	Remap → DiffSearch → Remap → ParamAdapt (FNA)	133.03	**33.9**
(3)	Remap → RandSearch → Remap → ParamAdapt	133.11	33.5
(4)	RandInit → RandSearch → Remap → ParamAdapt	133.08	31.5
(5)	Remap → RandSearch → RandInit → ParamAdapt	133.11	25.3
(6)	RandInit → RandSearch → RandInit → ParamAdapt	133.08	24.9

4.4 Random Search Experiments

We carry out the Random Search (RandSearch) experiments with the RetinaNet (Lin et al., 2017) framework on the MS-COCO (Lin et al., 2014a) dataset. All the results are shown in the Tab. 6. We purely replace the original differentiable NAS (DiffSearch) method in FNA with the random search method in Row (3). The random search takes the same computation cost as the search in FNA for fair comparisons. We observe that FNA with RandSearch achieves comparable results with

our original method. It further confirms that FNA is a general framework for network adaptation and has great generalization. NAS is only an implementation tool for architecture adaptation. The whole framework of FNA can be treated as a NAS-method agnostic mechanism. It is worth noting that even using random search, our FNA still outperforms DetNAS (Chen et al., 2019b) with 0.2% mAP better and 150M MAdds fewer.

We further conduct similar ablation studies with experiments in Sec. 4.3 about the parameter remapping scheme in Row (4) - (6). All the experiments further support the effectiveness of the parameter remapping scheme.

4.5 STUDY ON PARAMETER REMAPPING

We explore more strategies for the Parameter Remapping paradigm. Similar to Sec. 4.3, all the experiments are conducted with the DeepLabv3 (Chen et al., 2017b) framework on the Cityscapes dataset (Cordts et al., 2016). We make exploration from the following respects. For simplicity, we denote the weights of the seed network and the new network on the remapping dimension (output/input channel) as $\boldsymbol{W}_s = (\boldsymbol{W}_s^{(1)} \ldots \boldsymbol{W}_s^{(p)})$ and $\boldsymbol{W}_n = (\boldsymbol{W}_n^{(1)} \ldots \boldsymbol{W}_n^{(q)})$, where $q \leq p$.

Remapping with BN Statistics on Width-level   We review the formulation of batch normalization (Ioffe & Szegedy, 2015) as follows,

$$y_i \leftarrow \gamma \frac{x_i - \mu_{\mathcal{B}}}{\sqrt{\sigma_{\mathcal{B}}^2 + \epsilon}} + \beta, \tag{5}$$

where $x_i = (x_i^{(1)} \ldots x_i^{(p)})$ denotes the p-dimensional input tensor of the ith layer, $\gamma \in \mathbb{R}^p$ denotes the learnable parameter which scales the normalized data on the channel dimension. We compute the absolute values of γ as $|\gamma| = (|\gamma^{(1)}| \ldots |\gamma^{(p)}|)$. When remapping the parameters on the width-level, we sort the values of $|\gamma|$ and map the parameters with the sorted top-q indices. More specifically, we define a weights remapping function in Algo. 1, where the reference vector $\boldsymbol{v}$ is $|\gamma|$.

Algorithm 1: Weights Remapping Function

Input: the seed weights $\boldsymbol{W}_s$ and the new weights $\boldsymbol{W}_n$, the reference vector $\boldsymbol{v}$
1 // get indices of topk values of the vector
2 $\boldsymbol{a} \leftarrow topk\text{-}indices(\boldsymbol{v}, k = q)$
3 // sort the indices
4 $sort(\boldsymbol{a})$
5 **for** $i \in 1, 2, \ldots, q$ **do**
6 $\quad \boldsymbol{W}_n^{(i)} = \boldsymbol{W}_s^{(\boldsymbol{a}[i])}$
7 **end**
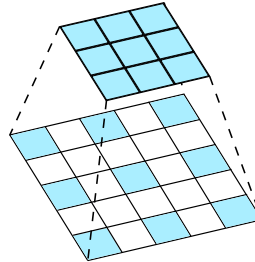**Output:** $\boldsymbol{W}_n$ with remapped values

Figure 3: Parameter Remapping on the kernel-level with a dilation setting.

Remapping with Weight Importance on Width-level   We attempt to utilize a canonical form of convolution weights to measure the importance of parameters. Then we remap the seed network parameters with great importance to the new network. The remapping operation is conducted based on Algo. 1 as well. We experiment with two canonical forms of weights to compute the reference vector, the standard deviation of $\boldsymbol{W}_s$ as $(std(\boldsymbol{W}_s^{(1)}) \ldots std(\boldsymbol{W}_s^{(p)}))$ and the L^1 norm of $\boldsymbol{W}_s$ as $(||\boldsymbol{W}_s^{(1)}||_1 \ldots ||\boldsymbol{W}_s^{(p)}||_1)$.

Table 7: Study the methods of Parameter Remapping.

Method	Width-BN	Width-Std	Width-L1	Kernel-Dilate	FNA
mIOU(%)	75.8	75.8	75.3	75.6	**76.6**

Remapping with Dilation on Kernel-level   We experiment with another strategy of parameter remapping on the kernel-level. Different from the function-preserving method defined in Sec. 3.1, we remap the parameters with a dilation manner as shown in Fig. 3. The values in the convolution

kernel without remapping are all assigned as 0. It is formulated as

$$\boldsymbol{W}^{k \times k}_{:,:,h,w} = \begin{cases} \boldsymbol{W}^{3 \times 3}_{:,:,h,w} & \text{if } h, w = 1 + i \cdot \frac{k-1}{2} \text{ and } i = 0, 1, 2 \\ 0 & \text{otherwise} \end{cases}, \tag{6}$$

where $\boldsymbol{W}^{k \times k}$ and $\boldsymbol{W}^{3 \times 3}$ denote the weights of the new network and the seed network respectively, h, w denote the spatial indices.

Tab. 7 shows the experimental results. The network adaptation with the parameter remapping paradigm define in FNA achieves the best results. Furthermore, the remapping operation of FNA is easier to implement compared to the several aforementioned ones. However, we explore limited number of methods to implement the parameter remapping paradigm. How to conduct the remapping strategy more efficiently remains a significative future work.

5 CONCLUSION

In this paper, we propose a fast neural network adaptation method (FNA) with a parameter remapping paradigm and the architecture search method. We adapt the manually designed network MobileNetV2 to semantic segmentation and detection tasks on both architecture- and parameter- level. The parameter remapping strategy takes full advantages of the seed network parameters, which greatly accelerates both the architecture search and parameter fine-tuning process. With our FNA method, researchers and engineers could fast adapt more manually designed networks to various frameworks on different tasks. As there are lots of ImageNet pre-trained models available in the community, we could conduct adaptation with low cost and do more applications, e.g., face recognition, pose estimation, depth estimation, etc. We leave more efficient remapping strategies and more applications for future work.

REFERENCES

Gabriel Bender, Pieter-Jan Kindermans, Barret Zoph, Vijay Vasudevan, and Quoc V. Le. Understanding and simplifying one-shot architecture search. In *ICML*, 2018.

Andrew Brock, Theodore Lim, James M. Ritchie, and Nick Weston. SMASH: one-shot model architecture search through hypernetworks. *arXiv:1708.05344*, 2017.

Han Cai, Tianyao Chen, Weinan Zhang, Yong Yu, and Jun Wang. Efficient architecture search by network transformation. In *AAAI*, 2018.

Han Cai, Ligeng Zhu, and Song Han. ProxylessNAS: Direct neural architecture search on target task and hardware. In *ICLR*, 2019.

Kai Chen, Jiaqi Wang, Jiangmiao Pang, Yuhang Cao, Yu Xiong, Xiaoxiao Li, Shuyang Sun, Wansen Feng, Ziwei Liu, Jiarui Xu, Zheng Zhang, Dazhi Cheng, Chenchen Zhu, Tianheng Cheng, Qijie Zhao, Buyu Li, Xin Lu, Rui Zhu, Yue Wu, and Dahua Lin. Mmdetection: Open mmlab detection toolbox and benchmark. *arXiv:1906.07155*, 2019a.

Liang-Chieh Chen, George Papandreou, Iasonas Kokkinos, Kevin Murphy, and Alan L Yuille. Deeplab: Semantic image segmentation with deep convolutional nets, atrous convolution, and fully connected crfs. *TPAMI*, 2017a.

Liang-Chieh Chen, George Papandreou, Florian Schroff, and Hartwig Adam. Rethinking atrous convolution for semantic image segmentation. *arXiv:1706.05587*, 2017b.

Liang-Chieh Chen, Maxwell D. Collins, Yukun Zhu, George Papandreou, Barret Zoph, Florian Schroff, Hartwig Adam, and Jonathon Shlens. Searching for efficient multi-scale architectures for dense image prediction. In *NeurIPS*, 2018a.

Liang-Chieh Chen, Yukun Zhu, George Papandreou, Florian Schroff, and Hartwig Adam. Encoder-decoder with atrous separable convolution for semantic image segmentation. In *ECCV*, 2018b.

Tianqi Chen, Ian J. Goodfellow, and Jonathon Shlens. Net2net: Accelerating learning via knowledge transfer. *arXiv:1511.05641*, 2015.

Yukang Chen, Tong Yang, Xiangyu Zhang, Gaofeng Meng, Chunhong Pan, and Jian Sun. Detnas: Neural architecture search on object detection. In *NeurIPS*, 2019b.

Marius Cordts, Mohamed Omran, Sebastian Ramos, Timo Rehfeld, Markus Enzweiler, Rodrigo Benenson, Uwe Franke, Stefan Roth, and Bernt Schiele. The cityscapes dataset for semantic urban scene understanding. In *CVPR*, 2016.

Jia Deng, Wei Dong, Richard Socher, Li-Jia Li, Kai Li, and Fei-Fei Li. Imagenet: A large-scale hierarchical image database. In *CVPR*, 2009.

Thomas Elsken, Jan Hendrik Metzen, and Frank Hutter. Efficient multi-objective neural architecture search via lamarckian evolution. In *ICLR*, 2019.

Jiemin Fang, Yukang Chen, Xinbang Zhang, Qian Zhang, Chang Huang, Gaofeng Meng, Wenyu Liu, and Xinggang Wang. EAT-NAS: elastic architecture transfer for accelerating large-scale neural architecture search. *arXiv:1901.05884*, 2019a.

Jiemin Fang, Yuzhu Sun, Qian Zhang, Yuan Li, Wenyu Liu, and Xinggang Wang. Densely connected search space for more flexible neural architecture search. *arXiv:1906.09607*, 2019b.

Kaiming He, Xiangyu Zhang, Shaoqing Ren, and Jian Sun. Deep residual learning for image recognition. In *CVPR*, 2016.

Kaiming He, Ross B. Girshick, and Piotr Dollár. Rethinking imagenet pre-training. *arXiv:1811.08883*, 2018.

Andrew G. Howard, Menglong Zhu, Bo Chen, Dmitry Kalenichenko, Weijun Wang, Tobias Weyand, Marco Andreetto, and Hartwig Adam. Mobilenets: Efficient convolutional neural networks for mobile vision applications. *arXiv:1704.04861*, 2017.

Gao Huang, Zhuang Liu, Laurens van der Maaten, and Kilian Q. Weinberger. Densely connected convolutional networks. In *CVPR*, 2017.

Sergey Ioffe and Christian Szegedy. Batch normalization: Accelerating deep network training by reducing internal covariate shift. In *ICML*, 2015.

Diederik P. Kingma and Jimmy Ba. Adam: A method for stochastic optimization. In *ICLR*, 2015.

Alex Krizhevsky, Ilya Sutskever, and Geoffrey E. Hinton. Imagenet classification with deep convolutional neural networks. In *NeurIPS*, 2012.

Zeming Li, Chao Peng, Gang Yu, Xiangyu Zhang, Yangdong Deng, and Jian Sun. Detnet: Design backbone for object detection. In *ECCV*, 2018.

Tsung-Yi Lin, Michael Maire, Serge J. Belongie, James Hays, Pietro Perona, Deva Ramanan, Piotr Dollár, and C. Lawrence Zitnick. Microsoft COCO: common objects in context. In *ECCV*, 2014a.

Tsung-Yi Lin, Michael Maire, Serge J. Belongie, James Hays, Pietro Perona, Deva Ramanan, Piotr Dollár, and C. Lawrence Zitnick. Microsoft COCO: common objects in context. In *ECCV*, 2014b.

Tsung-Yi Lin, Priya Goyal, Ross Girshick, Kaiming He, and Piotr Dollár. Focal loss for dense object detection. In *ICCV*, 2017.

Chenxi Liu, Barret Zoph, Maxim Neumann, Jonathon Shlens, Wei Hua, Li-Jia Li, Li Fei-Fei, Alan L. Yuille, Jonathan Huang, and Kevin Murphy. Progressive neural architecture search. In *ECCV*, 2018.

Chenxi Liu, Liang-Chieh Chen, Florian Schroff, Hartwig Adam, Wei Hua, Alan L Yuille, and Li Fei-Fei. Auto-deeplab: Hierarchical neural architecture search for semantic image segmentation. In *CVPR*, 2019a.

Hanxiao Liu, Karen Simonyan, and Yiming Yang. DARTS: Differentiable architecture search. In *ICLR*, 2019b.

Wei Liu, Dragomir Anguelov, Dumitru Erhan, Christian Szegedy, Scott Reed, Cheng-Yang Fu, and Alexander C Berg. Ssd: Single shot multibox detector. In *ECCV*, 2016.

Zili Liu, Tu Zheng, Guodong Xu, Zheng Yang, Haifeng Liu, and Deng Cai. Training-time-friendly network for real-time object detection. *arXiv:1909.00700*, 2019c.

Jonathan Long, Evan Shelhamer, and Trevor Darrell. Fully convolutional networks for semantic segmentation. In *CVPR*, 2015.

Ilya Loshchilov and Frank Hutter. SGDR: stochastic gradient descent with warm restarts. In *ICLR*, 2017.

Ningning Ma, Xiangyu Zhang, Hai-Tao Zheng, and Jian Sun. Shufflenet V2: practical guidelines for efficient CNN architecture design. In *ECCV*, 2018.

Hieu Pham, Melody Y. Guan, Barret Zoph, Quoc V. Le, and Jeff Dean. Efficient neural architecture search via parameter sharing. In *ICML*, 2018.

Esteban Real, Alok Aggarwal, Yanping Huang, and Quoc V. Le. Regularized evolution for image classifier architecture search. *arXiv:abs/1802.01548*, 2018.

Shaoqing Ren, Kaiming He, Ross B. Girshick, and Jian Sun. Faster R-CNN: towards real-time object detection with region proposal networks. *NeurIPS*, 2015.

Olaf Ronneberger, Philipp Fischer, and Thomas Brox. U-net: Convolutional networks for biomedical image segmentation. In *LNCS*, 2015.

Mark Sandler, Andrew Howard, Menglong Zhu, Andrey Zhmoginov, and Liang-Chieh Chen. Mobilenetv2: Inverted residuals and linear bottlenecks. In *Proceedings of the IEEE Conference on Computer Vision and Pattern Recognition*, 2018.

Karen Simonyan and Andrew Zisserman. Very deep convolutional networks for large-scale image recognition. *arXiv:1409.1556*, 2014.

Christian Szegedy, Vincent Vanhoucke, Sergey Ioffe, Jonathon Shlens, and Zbigniew Wojna. Rethinking the inception architecture for computer vision. In *CVPR*, 2016.

Mingxing Tan, Bo Chen, Ruoming Pang, Vijay Vasudevan, and Quoc V. Le. Mnasnet: Platform-aware neural architecture search for mobile. *arXiv:1807.11626*, 2018.

Jingdong Wang, Ke Sun, Tianheng Cheng, Borui Jiang, Chaorui Deng, Yang Zhao, Dong Liu, Yadong Mu, Mingkui Tan, Xinggang Wang, Wenyu Liu, and Bin Xiao. Deep high-resolution representation learning for visual recognition. *arXiv:1908.07919*, 2019.

Robert J Wang, Xiang Li, and Charles X Ling. Pelee: A real-time object detection system on mobile devices. In *NeurIPS*, 2018.

Bichen Wu, Xiaoliang Dai, Peizhao Zhang, Yanghan Wang, Fei Sun, Yiming Wu, Yuandong Tian, Peter Vajda, Yangqing Jia, and Kurt Keutzer. Fbnet: Hardware-aware efficient convnet design via differentiable neural architecture search. *arXiv:1812.03443*, 2018.

Changqian Yu, Jingbo Wang, Chao Peng, Changxin Gao, Gang Yu, and Nong Sang. Bisenet: Bilateral segmentation network for real-time semantic segmentation. In *ECCV*, 2018.

Fisher Yu and Vladlen Koltun. Multi-scale context aggregation by dilated convolutions. In *ICLR*, 2016.

Yiheng Zhang, Zhaofan Qiu, Jingen Liu, Ting Yao, Dong Liu, and Tao Mei. Customizable architecture search for semantic segmentation. In *CVPR*, 2019.

Barret Zoph and Quoc V. Le. Neural architecture search with reinforcement learning. *arXiv:1611.01578*, 2016.

Barret Zoph, Vijay Vasudevan, Jonathon Shlens, and Quoc V. Le. Learning transferable architectures for scalable image recognition. *arXiv:1707.07012*, 2017.

A APPENDIX

A.1 IMPLEMENTATION DETAILS ON SEMANTIC SEGMENTATION

For architecture adaptation, the image is first resized to 512×1024 and 321×321 patches are randomly cropped as the input data. The output feature maps are down-sampled by the factor of 16. Depthwise separable convolutions are used in the ASPP module (Chen et al., 2017a;b). The stages where the expansion ratio of MBConv is 6 in the original MobileNetV2 are searched and adjusted. We set the maximum numbers of layers in each searched stage of the super network as $\{4, 4, 6, 6, 4, 1\}$. We set a warm-up stage in the first 5 epochs to linearly increase the learning rate from 1×10^{-4} to 0.02. Then, the learning rate decays to 1×10^{-3} with the cosine annealing schedule (Loshchilov & Hutter, 2017). The batch size is set as 16. We use the SGD optimizer with 0.9 momentum and 5×10^{-4} weight decay for operation weights and the Adam optimizer (Kingma & Ba, 2015) with 4×10^{-5} weight decay and a fixed learning rate 1×10^{-3} for architecture parameters.

For parameter adaptation, the training data is cropped as a 769×769 patch from the rescaled image. The scale is randomly selected from $[0.75, 1.0, 1.25, 1.5, 1.75, 2.0]$. The random left-right flipping is used. We update the statistics of the batch normalization (BN) (Ioffe & Szegedy, 2015) for 2000 iterations before the fine-tuning process. We use the same SGD optimizer as the search process. The learning rate linearly increases from 1×10^{-4} to 0.01 and then decays to 0 with the polynomial schedule. The batch size is set as 16.

A.2 IMPLEMENTATION DETAILS ON OBJECT DETECTION

RetinaNet We describe the details in the search process of architecture adaptation as follows. The depth settings in each searched stage are set as $\{4, 4, 4, 4, 4, 1\}$. For the input image size, the short side is resized to 800 while the maximum long side is set as 1333. For operation weights, we use the SGD optimizer with 1×10^{-4} weight decay and 0.9 momentum. We set a warm-up stage in the first 500 iterations to linearly increase the learning rate from 0 to 0.02. Then we decay the learning rate by a factor of 0.1 at the 8th and 11th epoch. For the architecture parameters, we use the Adam optimizer (Kingma & Ba, 2015) with 1×10^{-3} weight decay and a fixed learning rate 3×10^{-4}. For the multi-objective loss function, we set λ as 0.02 and τ as 10. We begin optimizing the architecture parameters after 8 epochs. We remove the random flipping operation on input images in the search process. All the other training settings are the same as MMDetection (Chen et al., 2019a) implementation.

For fine-tuning of the parameter adaptation, we use the SGD optimizer with 5×10^{-5} weight decay and 0.9 momentum. A similar warm-up procedure is set in the first 500 iterations to increase the learning rate from 0 to 0.05. Then we decay the learning rate by 0.1 at the 8th and 11th epoch. The whole architecture search process takes 14 epochs, 18 hours on 8 TITAN-Xp GPUs with the batch size of 8 and the whole parameter fine-tuning takes 12 epochs, 10 hours on 8 TITAN-Xp GPUs with 32 batch size.

SSDLite We resize the input images to 320×320. For operation weights in the search process, we use the standard RMSProp optimizer with 4×10^{-5} weight decay. The warm-up stage in the first 500 iterations increases learning rate from 0 to 0.03. Then we decay the learning rate by 0.1 at 16 and 22 epochs. The architecture optimization starts at 12 epochs. We set λ as 0.2 and τ as 10 for the loss function. The other search settings are the same as the RetinaNet experiment.

For parameter adaptation, the initial learning rate is 0.2 and decays at 36, 50 and 56 epochs. The training settings follow the SSD (Liu et al., 2016) implementation in MMDetection (Chen et al., 2019a). The search process takes 24 epochs in total, 20 hours on 8 TITAN-Xp GPUs with 64 batch size. The parameter adaptation takes 60 epochs, 46 hours on 8 TITAN-Xp GPUs with 512 batch size.
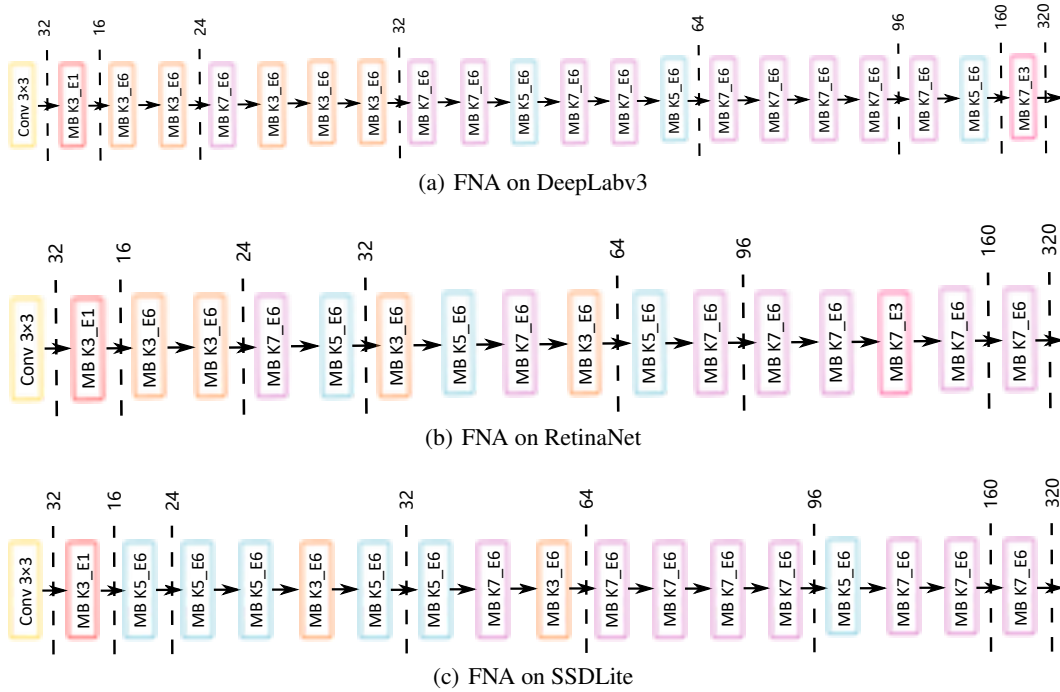

(a) FNA on DeepLabv3

(b) FNA on RetinaNet

(c) FNA on SSDLite

Figure 4: Visualization of our searched architectures on different frameworks. MB: inverted residual block proposed in MobilenetV2 (Sandler et al., 2018). Kx_Ey: the kernel size of the depthwise convolution is x and the expansion ratio is y.
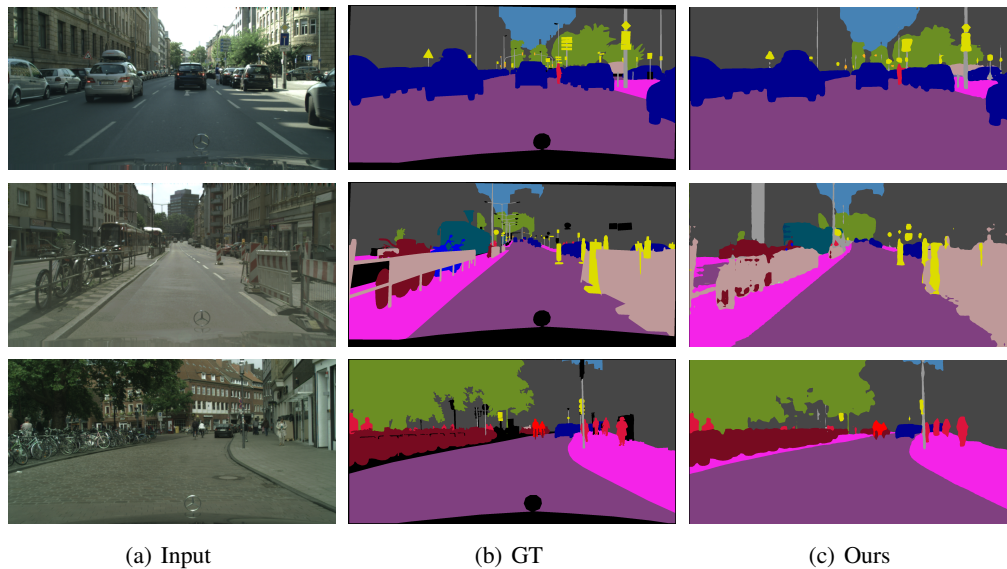

(a) Input   (b) GT   (c) Ours

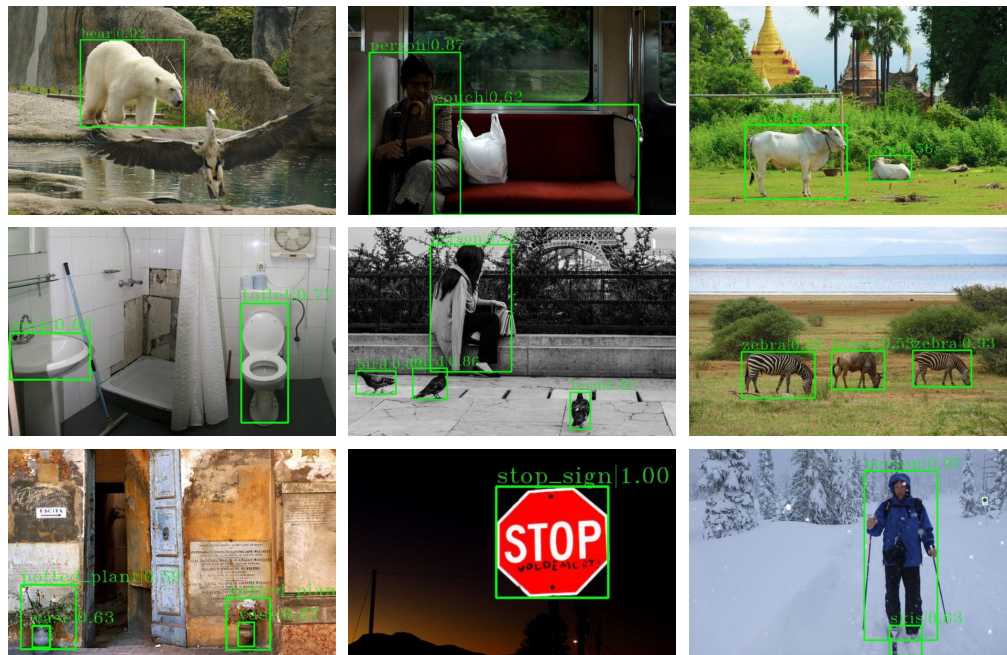Figure 5: Visualization of semantic segmentation results on the Cityscapes validation dataset.

Figure 6: Visualization of object detection results on the MS-COCO validation dataset.